

Article

Determination of the Variation of the Geometric and Dynamic Parameters of the Floodplain Vegetation

Natalia Walczak ^{1,*}, Zbigniew Walczak ² and Tomasz Ficner ¹

¹ Department of Hydraulic and Sanitary Engineering, Poznan University of Life Sciences, 60-637 Poznan, Poland; nwalczak@up.poznan.pl

² Department of Construction and Geoengineering, Poznan University of Life Sciences, 60-637 Poznan, Poland; zbigniew.walczak@up.poznan.pl

* Correspondence: natalia.walczak@up.poznan.pl

Abstract: Floodplain vegetation is characterized by its ability to resist deformation and destruction and to deform elastically and plastically under the influence of external mechanical forces. The force of water that presses on the plant induces stress and deformation in it, but once the force is removed, the elastic properties of the vegetation return it to its original state. It regains its original size, shape, and volume. In this paper, the deflection arrow was analysed based on the field tests conducted, and then the modulus of elasticity of natural shrub vegetation was determined. Measurements were made at different plant heights. Analysis was carried out at different growing periods to estimate the variation of plant elasticity with growth, development, and season. The results confirm the loss of flexibility during winter for all the shrubs analysed. Based on the measurements carried out, the elastic modulus E of the shoots was estimated. The average modulus of elasticity ranged from about 2100 to about 4000 MPa and showed high variability, reaching even $\mu = 50\%$, both within a given shrub and depending on the measurement season. The results presented here indicate a high natural variability of mechanical parameters even within the same plant.



Citation: Walczak, N.; Walczak, Z.; Ficner, T. Determination of the Variation of the Geometric and Dynamic Parameters of the Floodplain Vegetation. *Water* **2022**, *14*, 1274. <https://doi.org/10.3390/w14081274>

Academic Editor:
Francesco Gallerano

Received: 11 March 2022

Accepted: 12 April 2022

Published: 14 April 2022

Publisher's Note: MDPI stays neutral with regard to jurisdictional claims in published maps and institutional affiliations.



Copyright: © 2022 by the authors. Licensee MDPI, Basel, Switzerland. This article is an open access article distributed under the terms and conditions of the Creative Commons Attribution (CC BY) license (<https://creativecommons.org/licenses/by/4.0/>).

Keywords: shrubby vegetation; modulus of elasticity; deflection arrow of the plant; vegetations

1. Introduction

Rivers and their floodplains provide a resource for many different ecosystems that depend on the availability of water. The channel zone is the habitat of many species of flora and fauna, including plankton, various vertebrates, invertebrates, and macrophytes. Floodplains, on the other hand, can provide both valuable natural habitats, through the formation of ecologically diverse riparian communities [1], and economic or agricultural habitats as a result of, among other things, the abundance of meadows, which can be a source of food for grazing animals [2]. However, vegetation also increases hydraulic roughness and reduces the effective flow area, causing an increase in water surface elevation for the same flow. Balancing the desire to preserve vegetation in valley areas with the need to manage flood risk requires the use of accurate techniques to predict the effects of vegetation on water hydraulics [3].

Sustained and ongoing access to water is particularly important during periods of increased climate change, where emerging periods of drought can be interspersed with localised flooding or waterlogging resulting from intense and/or heavy rains. Floodplain vegetation should function well, both under conditions of high soil moisture and rising groundwater levels and during prolonged droughts. Unrestricted access to water results in intensive growth of vegetation, which is an important natural and economic element, but unfortunately during floods it can influence the hydraulic conditions by, among other things, reducing the cross-sectional area of the river. Therefore, information on the growth rate and variability of floodplain vegetation's geometry and hydrodynamic properties over time is of great importance for flood protection.

The effect of plants on flow conditions depends largely on hydrodynamic parameters, i.e., the type of plants, their growth stage, geometric and mechanical characteristics. One of the most important mechanical characteristics is the elasticity of plants. This feature causes plants to deform to varying degrees as a result of the flowing water acting on them. Among other things, the size of the modulus of elasticity determines how much force is required for deflection to occur. The knowledge of this parameter, especially in the case of flexible vegetation in the inter-bank area (wicker shrubs, alders, reeds, etc.), is of great importance in predicting the behaviour of the vegetation and determining hydrodynamic resistance.

Concerning the arrangement of the water table and geometric dimensions, biological developments can be divided into low vegetation, whose height is several times lower than the height of the water table, e.g., low grasses; medium vegetation, whose height is approximately equal to the height of the water table, e.g., tall grasses, shrubs; and high vegetation, which is significantly higher than the height of the water table, e.g., tall shrubs, trees. The imperfection of this division is that vegetation classification depends on the water table, which can vary depending on the hydrological conditions in the river. However, it is important because, depending on how submerged the vegetation is, its effect on water flow is estimated differently. Completely submerged vegetation is most often characterised by the absolute roughness coefficient k_s [4]. On the other hand, the influence of non-submerged vegetation is mainly related to the roughness resulting from water flowing around plant bodies, which requires the determination of geometrical characteristics and their spatial distribution in the floodplain [4].

Another division of floodplain vegetation can be made taking into account environmental conditions, including water and air conditions in the soil or substrate. Then we distinguish, according to [5], submerged or floating vegetation (hydrophytes), which is characterised by a lack of lignified tissues and high resilience, and emerged vegetation (helophytes), which is characterised by greater rigidity but has the capability of elastic deflection depending on water pressure. The last vegetation type in this category is vegetation consisting of species adapted to high water levels in the ground and periodic flooding, and thus complete saturation of the soil with water.

The biological structure of river valleys can also be divided taking into account the behaviour of plants (deflection) against the hydrodynamic pressure of flowing water [4]. In this case, we distinguish rigid plants, which are characterised by the absence of deformation, e.g., trees; elastic plants, which undergo elastic deformation, e.g., tall grasses, shrubs; and smooth plants, represented by most submerged plants which are characterised by permanent deformation.

Of these three types of vegetation, only rigid and smooth vegetation has been satisfactorily described in terms of their deflection characteristics. On the contrary, resilient vegetation and the flow resistance induced by it have not been fully investigated, mainly due to the influence of varying biomechanical parameters of plants depending on species, growing season, and the hydrodynamic force of water pressure [4].

Aquatic plants are a common component of many environments, including rivers, flood plains, coastal regions and shallow lakes. They ensure the proper functioning of environmental ecosystems, such as producing and storing carbon [6,7], increasing bottom and slope stability [8,9], and providing shelter [10] and food [11] for fish and aquatic invertebrates. Aquatic plants can be adversely affected by flows at high water levels by inducing pressure forces that can damage them [12] or uproot them [13]. Flexible plants can reduce their exposure to resistance by bending in response to water flow, a process known as reconfiguration [14], by which the roughness of the riverbank increases and the drainage capacity of riverbeds is reduced [15–17].

The growth rate of riparian trees is crucial for their ability to actively participate in river channel dynamics [18,19]. The researchers analysed a 21 km section of the Tagliamento River in Italy. In the research, archival and actual airborne lidar, colour air photographs, and ground measurements to determine whether colonization of exposed river sediments by riparian trees has an impact on fluvial dynamics and the evolution of fluvial landforms'

channel form and to quantify any impact that is identified. The use of combined measurement techniques in all analyses has allowed for the estimation of a set of morphological and vegetation properties at high spatial resolution over a sizeable reach of a braided gravel bed river where vegetation colonization and growth interact freely with fluvial processes. The researchers confirmed that it is possible to combine historical remote sensing datasets with non-synchronous and diverse terrestrial observations using mainly freely available software to obtain information of sufficient quality to test basic scientific hypotheses, in particular, to analyse how riparian tree growth affects the morphological structure of braided river sections under conditions where other factors such as peak flow rate, slope and grain size remain approximately constant.

Similarly, Džubáková et al. [20] analysed the possibility of applying terrestrial photography to the monitoring of riparian vegetation response to flood disturbances. The research included a field study of the floodplain of the river Maggia, which is an Alpine located in southeastern Switzerland, north of the city of Locarno. Basic vegetation indices (VIs) were analysed. The analysis period included five floods between 2008 and 2011. The results confirmed a negative (destruction) but also positive (enhancement) response of the vegetation within one week after the flood, with the response depending on the vigour of the vegetation before the flood, the geomorphological conditions and the intensity of the flood forcing. The response of floodplain vegetation to the passage of a flood wave can vary significantly depending on the development environment. At the same time, the authors confirmed that the response of vegetation to flood disturbance can be effectively monitored using ground-based photography with near-infrared sensitivity, with potential relevance for long-term assessment in river management and restoration projects. Such monitoring is a valuable, low-cost alternative to continuous, repeated measurement and analysis of changes in river environments.

Riparian vegetation can also be a good indicator to investigate the link between the riparian areas and the bankfull discharge. Apollonio et al. [21] in their analyses used combined topographic observations and vegetation surveys with hydrological-hydraulic analysis in the Rio Torbido River, in central Italy, in order to confirm a possible correlation between the colonization of the riverbank by woody riparian species and the bankfull discharge. The researchers indicated that the vegetation, depending on the hydraulic conditions and the water table level, can be divided into three classes indicating their representatives. This vegetation can also be an indicator of riparian areas.

Velocity distribution is strongly influenced by the presence of vegetation. Such a study was conducted by, among others [22], who observed that under conditions of dense bank vegetation there is a concentration of flow in the main channel and a significant rise in water level. The study was conducted on a 300 m section of a drainage channel in an agricultural area. The authors confirmed that flow resistance decreases with increasing velocity, suggesting a significant effect of vegetation reconfiguration due to resistance. The studies by [22] may provide additional information for floodplain restoration practitioners because commonly used hydraulic design models do not account for the spatial variability of natural vegetation along the cross-section.

The configuration of the plant depends on the stiffness and density of the material. Natural plants exhibit a wide range of hydrodynamic characteristics, from highly flexible seagrass, which bends easily in weak streams, to reeds, whose greater stiffness limits bending except in very strong streams.

Many flexible aquatic plants deform under the force of water, resulting in a reduction in the resistance of the plant, both by reducing the frontal area and by creating a more streamlined shape. Zhang and Nepf [23] carried out such a study, measuring the resistance and position of individual plants in the laboratory over a range of flow velocities in the channel between 2 and 62 cm·s⁻¹. In the theoretical model, the authors determined plant resistance based on a balance of forces that included buoyancy force, restoring force due to stem stiffness and leaf resistance. The effect of foliage was characterised by the coefficient C_s , which was a function of leaf angle (as a deviation from vertical between 30–110 degrees),

leaf spacing, and leaf width. After validation, the model was used to investigate the effect of leaf configuration, following examples of natural vegetation. Modelling and experiments showed that resistance increased as the plant configuration changed (the highest resistance occurs for vertical plants and the lowest for horizontal plants).

Many previous studies concerned the determination of leaf resistance strength and its contribution to total resistance, e.g., measurements by Vogel [24] confirmed that single broad leaves, especially those with long petioles and bilaterally lobed or heart-shaped epiphyse, significantly reduce their resistance under the influence of strong winds ($10\text{--}20\text{ m}\cdot\text{s}^{-1}$). Similar conclusions were reached by [25–28], who concluded, based on their analysis, that the foliage significantly affects the resistance value, but may depend on the water speed. Jalonen and Järvelä [26], based on their study, found that leaf-induced resistance can account for up to 80% of the total resistance at low water velocity ($0.1\text{ m}\cdot\text{s}^{-1}$) and only up to 40% when the velocity exceeds $0.8\text{ m}\cdot\text{s}^{-1}$. Whittaker et al. [27] observed that the contribution of leaves to the amount of resistance varied depending on the plant species. Black alder (*Alnus glutinosa*) leaves contribute to 75% of the total resistance, while white willow (*Salix alba*) leaves contribute 30%.

Measurements of plant stability were carried out, among others, by Henry and Thomas [29], who studied the effect of lateral shading resulting from the proximity of other plants and wind on the growth of stems of the common weevil (*Abutilon theophrasti*) under laboratory conditions. The authors of the experiment found that the presence of other plants increases the height of the stem and root system, but decreases the diameter of the stem and leaf area. The stability of such plants is comparable to lower plants with smaller root systems that were not affected by wind and lateral shading.

The study of the resistance of water deflecting flexible vegetation under laboratory conditions was also carried out by Li, Xie and Su, [30]. The experiment included a combination of three flow velocities (V), three vegetation modulus of elasticity (E), and three vegetation shoot thicknesses (b). The results show that the bending of the vegetation helps to move the stem towards the bottom of the channel, which contributes to reducing the total flow resistance.

Recognition of the vegetation structure and determination of its parameters are a necessary condition for the construction of a reliable mathematical flow model. One of the most important mechanical characteristics of floodplain vegetation is elasticity. Knowledge of this parameter, especially in the case of flexible mid-floodplain vegetation, is important to determine the hydrodynamic resistance that plant communities place on flowing water. With this in mind, field studies of the deflection arrow and estimates of the elastic modulus of floodplain vegetation at different periods of their development were analysed using three different wicker shrubs as examples.

2. Materials and Methods

2.1. Description of the Research Object

Field measurements were carried out on 19 randomly selected branches of three shrubs located in the floodplain of the Warta River above Lech Bridge in Poznan (Figure 1) in three periods (vegetation periods 2020 and 2021 and non-vegetation periods 2020, Figures 2–4).

Shrub 1 (Figure 2) is located near the outlet of treated wastewater from the Aquanet SA treatment plant in Serbska Street, near Lech Bridge ($52^{\circ}25'48.697''\text{ N}$; $16^{\circ}57'55.042''\text{ E}$; 52.2 m a.s.l., approximately 7.5 m from the edge of the Warta riverbed). The shrub belongs to the species Brittle Willow (*Salix fragilis*) and is the smallest and also the youngest of all three shrubs. The spread of its crown at the widest point is about 5.0 m, while the height of the highest branches is about 3.9 m above ground level (measured on 14 July 2020).

Shrubs 2 and 3 (Figures 3 and 4) are located approximately 120 m away from shrub 1 following the flow of the Warta River ($52^{\circ}25'52.463''\text{ N}$; $16^{\circ}57'56.203''\text{ E}$, approximately 6.0 m from the Warta bank). The two shrubs are not far from each other and belong to the species Basket Willow (*Salix viminalis* L.) and White Willow (*Salix alba*), respectively. Shrub 2 is intermediate in size, and the spread of its crown at its widest point is approximately

5.9 m, while the height of the highest branches reaches approximately 3.7 m. Shrub no. 3 is the most spreading shrub and its crown at its widest point is approximately 9.0 m, while the height of its highest branches reaches approximately 4.7 m.

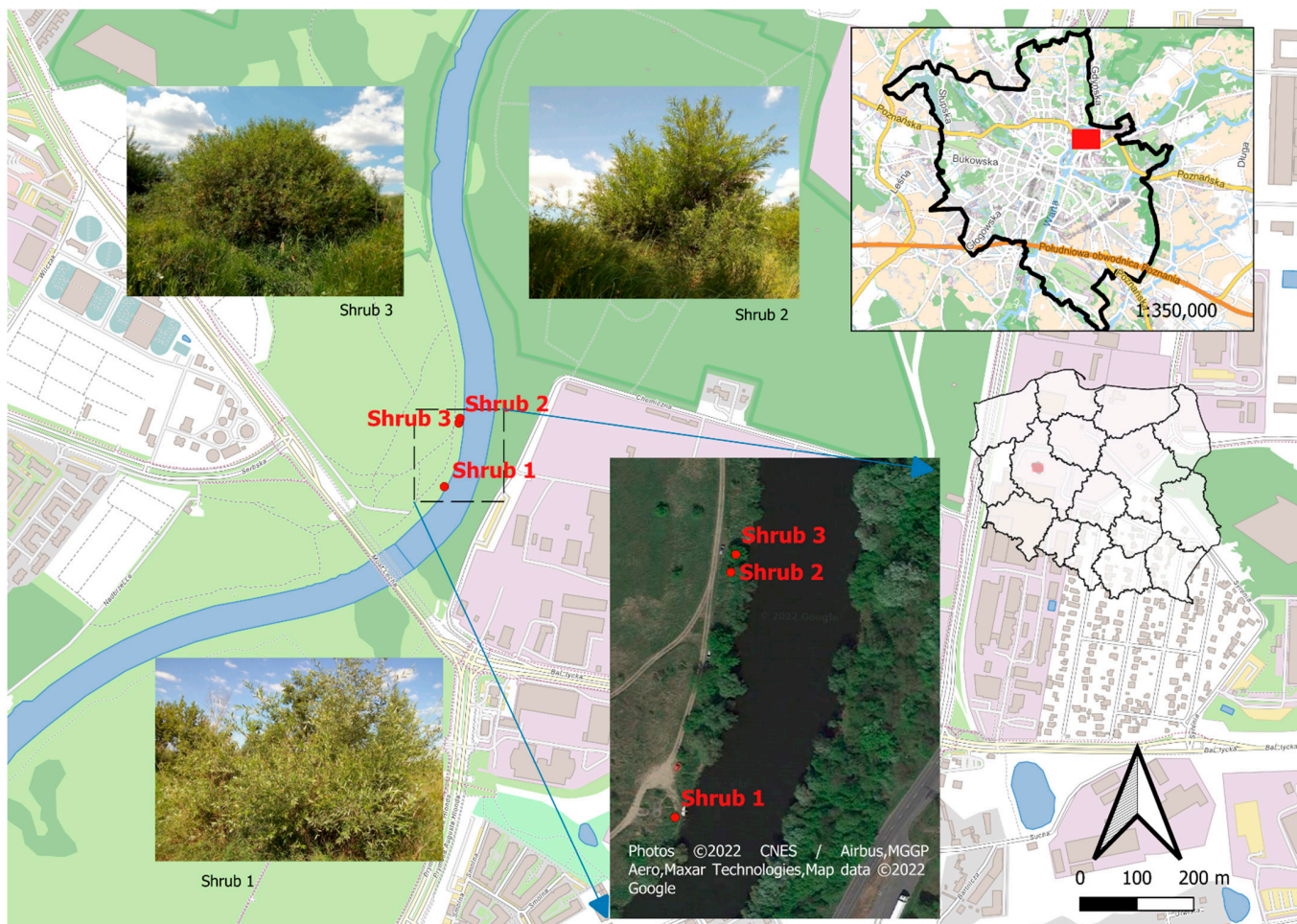


Figure 1. Illustrative map with locations of individual shrubs.



Figure 2. View of shrub 1 during the vegetation conditions ((left photo)—14 July 2020) and the non-vegetation conditions ((right photo)—13 December 2020).



Figure 3. View of shrub 2 during the vegetation conditions ((left photo)—14 July 2020) and the non-vegetation conditions ((right photo)—13 December 2020).



Figure 4. View of shrub 3 during the vegetation conditions ((left photo)—14 July 2020) and the non-vegetation conditions ((right photo)—13 December 2020).

2.2. Measurement of the Deflection Arrow

To determine the deflection arrow, the methodology of Tymiński et al. [31] was used, taking into account small and large deflections of flexible vegetation branches under the influence of concentrated force or hydrodynamic pressure loads acting on them. This methodology assumes that the shape of the branch is close to a truncated cone (Figure 5a–c).

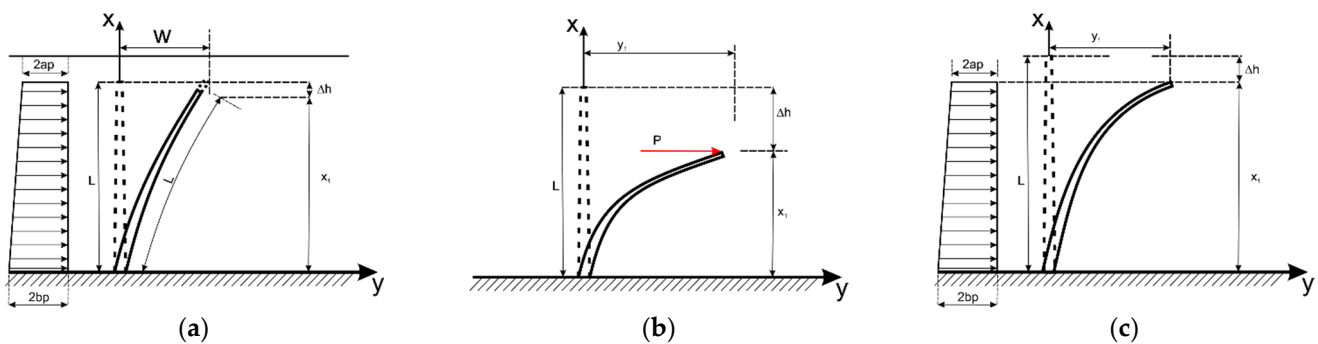


Figure 5. Calculation scheme of (a) small stem/branch truncated cone deflection loaded by hydrodynamic pressure (b) large stem/branch truncated cone or cylinder deflection loaded by concentrated force (c) large stem/branch truncated cone deflection loaded by hydrodynamic pressure (author’s figure based on [31], explanations in text).

For the case of a small truncated cone stem/branch deflection assuming a rectangular velocity distribution and a linearly varying stem/branch cross-sectional area, the hydrodynamic pressure distribution shown in Figure 5a was determined [31]:

$$y'' = \frac{3\lambda \cdot a \cdot (L-x)^2}{X^4} + \frac{\lambda \cdot (b-a) \cdot (L-x)^3}{L \cdot X^4} \quad (1)$$

$$\lambda = \frac{4p}{3\pi E} \quad (2)$$

$$X = (R-r) \cdot \left(1 - \frac{x}{L}\right) + r \quad (3)$$

$$p = \frac{1}{2} c_w \cdot \rho \cdot v^2 \quad (4)$$

where:

a, b —dimensions depending on stem/branch area [m],

L —original length of stem/branch [m],

x —stem/branch throw from the point of attachment [m],

λ —dimensionless coefficient of resistance [-],

p —external load, hydrodynamic pressure acting on the plant front surface [Pa],

R, r —initial and final radius of the stem/branch [m],

E —modulus of elasticity [Pa],

c_w —flow resistance coefficient [-],

ρ —water density [$\text{kg} \cdot \text{m}^{-3}$],

v —water velocity [$\text{m} \cdot \text{s}^{-1}$].

After a series of transformations and the integration of Equation (1) and the approximation that the deflection curve can be approximated by a parabola passing through a point with coordinates $x = L, y = w$, an equation allowing the determination of the deflection arrow can be obtained [31]:

$$1 = \frac{w \cdot x_1}{L^2} \cdot \sqrt{\frac{L^2}{4w^2} + \frac{x_1^2}{L^2}} + \frac{L}{2w} \cdot \sinh^{-1} \frac{w \cdot x_1}{L^2} \quad (5)$$

where:

w —deflection arrow [m] (Figure 1a),

x_1 —deflection height [m].

For large stem/branch deflections in cylindrical and truncated cone shapes, the basic equations are of the form:

$$y = \int_0^x \frac{u \, dx}{\sqrt{1-u^2}} \quad (6)$$

$$u = \int_0^x \varphi(x) \, dx \quad (7)$$

$$L = \int_0^{x_1} \frac{u \, dx}{\sqrt{1-u^2}} \quad (8)$$

where: $\varphi(x)$ —the load-dependent function for a cone-shaped stem/branch loaded with a concentrated force according to the scheme in Figure 5b can be determined from the equation [31]:

$$\varphi(x) = \frac{2k \cdot (x_1 - x)}{X^4} \quad (9)$$

$$X = (R-r) \cdot \left(1 - \frac{x}{x_1}\right) + r \quad (10)$$

$$k = \frac{2P}{\pi E} \quad (11)$$

$$u = \frac{2k \cdot (x_1 - x)^2}{(R - r)^2} \cdot \left(\frac{1}{3} \cdot \frac{r}{X^3} - \frac{1}{2X^2} - \frac{r}{3R^2} + \frac{1}{2R^2} \right) \quad (12)$$

where: P —the value of the concentrated force [N].

For a cone-shaped stem loaded by hydrodynamic pressure, the deflection arrow, according to the scheme in Figure 5c, can be determined from the equation [31]:

$$\varphi(x) = \frac{3\lambda a \cdot (x_1 - x)^2}{X^4} + \frac{\lambda \cdot (b - a) \cdot (x_1 - x)^3}{X_1 \cdot X^4} \quad (13)$$

$$X = (R - r) \cdot \left(1 - \frac{x}{x_1} \right) + r \quad (14)$$

$$\lambda = \frac{4P}{3\pi E} \quad (15)$$

In the case where $a = r$ and $b = R$:

$$u = \frac{\lambda \cdot (x_1 - x)^3}{(R - r)^3} \cdot \left(\ln \frac{X}{R} + \frac{3}{2} \frac{r^2}{X^2} - \frac{2r^3}{3X^3} - \frac{3}{2} \frac{r^2}{R^2} + \frac{2}{3} \frac{r^3}{R^3} \right) \quad (16)$$

In the case of both large deflections under concentrated force loading and hydrodynamic pressure loading, having the function describing the parameter u , it is possible to determine the value of x_1 from relation (8) and then the value of y from relation (6). Due to the complex forms of the functions that describe the parameter u , integrals (6) and (8) can be calculated using numerical integration methods [31].

The modulus of elasticity of the branches was determined using the formula for a cantilever beam with a truncated cone section:

$$E = \frac{64}{3} \cdot \frac{P \cdot l^3}{\pi \cdot w \cdot D^3 \cdot d} \quad (17)$$

where:

P —force induced by the load [N],

l —force arm [m],

w —size of deflection arrow [m],

D, d —larger and smaller diameter of the rod (branch) [m].

The field tests consisted in measuring the deflection of a randomly selected branch as a result of its being loaded with weights of 15, 30 and 50 g successively, and their multiples up to about 500 g, which corresponds approximately to loading the branches with flowing water with velocities in the range 0.09 to 1.8 m·s⁻¹. The loads for individual branches were applied at one of three levels: 50, 100, and 150 cm (Figure 6) above the ground. The level at which the load was applied to the branches depended on the position of a given shoot in the shrub and the position of the beginning of the branch relative to the ground level. For shrub 1, measurements were taken at 50 cm for three branches, 100 cm for two branches and 150 cm for three branches. For shrub 2, measurements were taken for three branches at the 50 cm level, one branch at the 100 cm level and three branches for the 150 cm level, respectively. While for shrub 3, measurements were taken for one branch at the 50 cm level, one branch at the 100 cm level and two branches at the 150 cm level, respectively. All loaded branches were inventoried in detail and the deflection measurement was always performed in the same place. The branches on which the measurements that were made were marked with labels at the place where the load was applied, and subsequent numbers of branches were marked. The measurement of the deflection arrow of individual branches was performed using a rack with a movable scale, allowing measurements within the range of approx. 20 to 160 cm above ground level (Figure 7).

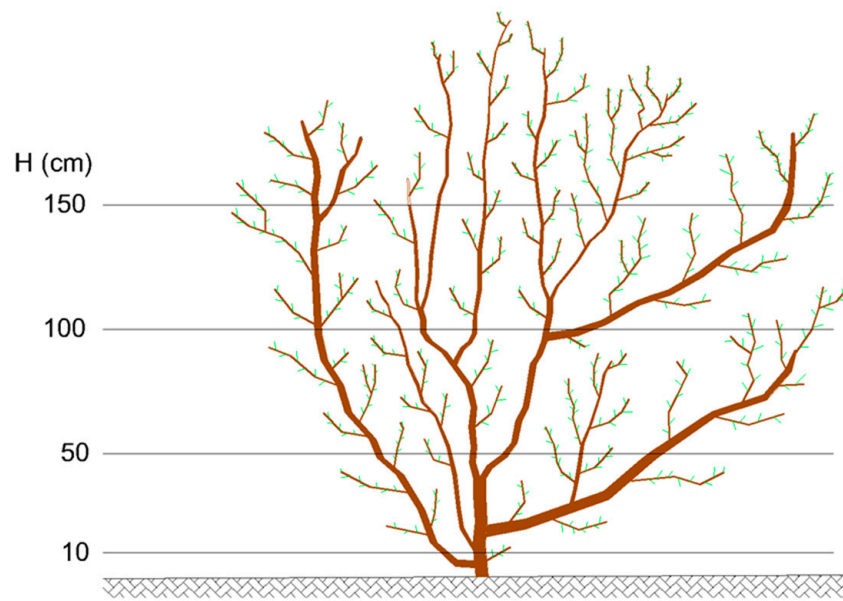


Figure 6. Diagram of the shrub with deflection measurement levels indicated.



Figure 7. Branch on shrub No. 3 during measurement of deflection arrow.

To evaluate the effect of the vegetation period and the ambient temperature on the elasticity of shrub branches, measurements of branch deflection arrows were made in two conditions: under vegetation periods (2020 and 2021) at an average air temperature of about 18 °C, and non-vegetation, winter conditions (2020) at an average air temperature of about 5 °C. The measurement under non-vegetation conditions was conducted in the snowmelt period after a long period (about two weeks) of negative temperatures. The obtained results of deflection arrows for individual loads were used to develop the modulus of elasticity

of individual branches using the equations for a cantilever beam with a truncated cone section loaded with a concentrated force (17).

2.3. Measurement of Diameters

Three measurement cycles of branch diameters were performed on individual shrubs. Two series of measurements were carried out during the growing season in 2020 and 2021 and one cycle of measurements during the non-vegetation conditions in 2020. Diameters were measured for each shrub at four levels: 10, 50, 100 and 150 cm above ground level. At each height, for each measurement cycle, between 30 and 70 randomly selected branches were measured (depending on the total number of branches at that height). The measurement was performed using an electronic caliper, with a measurement range of 0–150 mm and measurement accuracy of 0.01 mm. In the case of thick branches and trunks of shrubs (mainly shrub No. 3) with a diameter of more than 150 mm, the measurement was performed with a measuring tape with an accuracy of 1 mm. For all measurement series, for each of the four levels, the average diameter of the branches corresponding to each shrub was calculated.

3. Results

3.1. Branch Diameters

Measurements of branch diameters were carried out at four heights, 10, 50, 100 and 150 cm for each shrub in three periods: twice during the vegetation conditions in 2020 and 2021 and during the non-vegetation conditions in 2020. Summaries of the measurements are presented in Tables 1–3 and for shrub No. 3 in Figure 8. Changes in branch diameter between the vegetation periods and non-vegetation conditions are mainly due to changes in tension within the xylem [32]. Diurnal diameter changes [33,34] may result from, among other things, diurnal temperature changes or the influence of diurnal water changes [34]. The seasonal variation in diameter recorded in the measurements (Figure 8) is due to the occurrence of low temperatures [35–37] and the reduction of water and nutrient transport by the branches. The shrubs showed high variability in branch diameters μ ranging from about 33% to almost 90%, and standard deviation SD from 1.83 to almost 57.5 mm. Table 4 summarises the percentage change in the mean diameters of shrubs 1 and 3 between the vegetation conditions of 2020 and 2021. A fairly significant increase in diameter can be observed for shrub 3, which is located in the slope of the trough and thus closer to the groundwater table, which has a significant effect on the rate of diameter and branch growth. The average increase in branch diameter between 2020 and 2021 vegetation conditions for shrubs 1 and 3 ranged from 2 to 54%. In the literature, the average annual growth rate of willow branch diameters in later years of development is about 10–15% [38,39]. However, in the case of younger shrubs, this increment can be higher and reach up to 30% [40].

Table 1. Summary of the results of the series of measurements of the branches diameters of shrub No. 1.

Height above Ground Level (cm)	Season	Average Diameter (mm)	Standard Deviation σ (mm)	Coefficient of Variation μ (%)
10	under vegetation conditions 2020	14.69	10.90	74.2
	under non-vegetation2020	14.06	10.05	71.5
	under vegetation conditions 2021	15.89	11.01	69.3
50	under vegetation conditions 2020	8.20	5.41	66.0
	under non-vegetation2020	9.35	4.96	53.0
	under vegetation conditions 2021	8.56	3.48	40.6
100	under vegetation conditions 2020	7.51	4.09	54.4
	under non-vegetation 2020	6.79	4.44	65.3
	under vegetation conditions 2021	7.45	2.63	35.3
150	under vegetation conditions 2020	5.50	3.43	62.4
	under non-vegetation 2020	5.10	2.85	55.9
	under vegetation conditions 2021	5.64	1.83	32.5

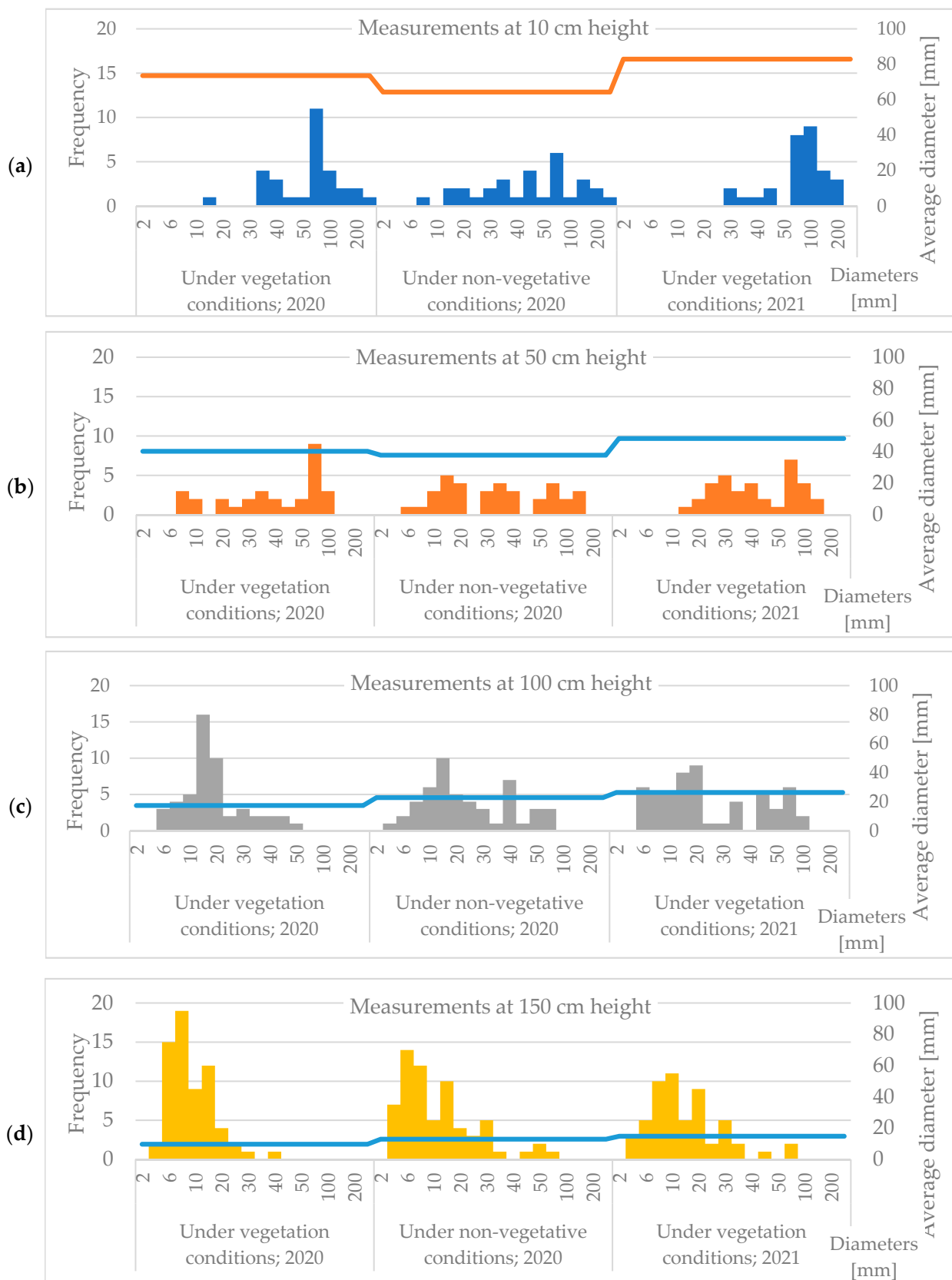


Figure 8. Histograms of No. 3 bush diameters. Measurements were taken at heights of (a) 10 cm, (b) 50 cm, (c) 100 cm, and (d) 150 cm above the ground.

Table 2. Summary of the results of the series of measurements of the branch diameters of shrub No. 2.

Height above Ground Level (cm)	Season	Average Diameter (mm)	Standard Deviation σ (mm)	Coefficient of Variation μ (%)
10	under vegetation conditions 2020	27.61	15.87	57.47
	under non-vegetation 2020	20.42	15.75	77.11
50	under vegetation conditions 2020	13.85	5.75	41.5
	under non-vegetation 2020	12.50	5.95	47.6
100	under vegetation conditions 2020	8.91	3.74	41.9
	under non-vegetation 2020	10.24	5.83	56.9
150	under vegetation conditions 2020	7.55	4.42	58.5
	under non-vegetation 2020	7.54	4.19	55.5

Table 3. Summary of the results of the series of measurements of the branches diameters of shrub No. 3.

Height above Ground Level (cm)	Season	Average Diameter (mm)	Standard Deviation σ (mm)	Coefficient of Variation μ (%)
10	under vegetation conditions 2020	73.58	52.51	71.4
	under non-vegetation 2020	64.29	57.45	89.4
	under vegetation conditions 2021	82.864	45.18	54.5
50	under vegetation conditions 2020	40.30	22.65	56.2
	under non-vegetation 2020	37.78	31.67	83.8
	under vegetation conditions 2021	48.36	30.38	62.8
100	under vegetation conditions 2020	17.31	10.74	62.1
	under non-vegetation 2020	22.78	16.42	72.1
	under vegetation conditions 2021	26.34	22.03	83.6
150	under vegetation conditions 2020	9.64	6.07	63.0
	under non-vegetation 2020	12.85	11.50	89.5
	under vegetation conditions 2021	14.80	11.41	77.1

Table 4. Summary of changes in mean diameters of shrubs 1 and 3 between the 2020 and 2021 vegetation seasons.

Height above Ground Level (cm)	Average Diameter Increment (%)	
	Shrub nr 1	Shrub nr 3
10	8	13
50	4	20
100	−1	52
150	2	54

3.2. Deflection Arrows

All lateral branches on which measurements were made were selected so that the minimum distance that the shoot started from the ground level was 0.5 m. Each shoot branch on which the deflection arrow measurements were performed was labelled (Figure 7) for unambiguous identification in subsequent measurement cycles. The branches were loaded successively with weights of 15, 30 and 50 g and multiples thereof at three heights, i.e., 50, 100 and 150 cm above ground level. Table 5 shows the measured deflection values and calculated modulus of elasticity, for example, branch No. 1 for shrub 1. Analogous analyses were conducted for the remaining branches and shrubs. The averaged values of the modulus of elasticity for individual branches for shrub No. 1 are summarised in Table 6. It was found that there was a loss of elasticity of the branches in the winter conditions and a decrease in deflection when the same load was applied concerning the growing conditions, which is related to the natural reaction of the plant in the non-vegetations period. The plant then enters a dormancy state, the foliage is lost and water and food requirements are

reduced. The apparent changes in deflection between the measuring conditions correspond to changes in diameter. Lignin concentration also increase during the winter season [41].

Table 5. Summary of deflection arrow measurements and calculated modulus of elasticity for branch No. 1 of shrub No. 1, for measurements at 50 cm height.

Branch No. 1 h = 50 cm							
Under Vegetation Conditions 2020				Under Non-Vegetation 2020/2021			
d_p * [mm]	5.84			d_p [mm]	5.04		
d_k [mm]	12.5			d_k [mm]	13.02		
L [cm]	120			L [cm]	120		
Z_o [cm]	12			Z_o [cm]	9		
G [g]	Z [cm]	Z' [cm]	E [MPa]	G [g]	Z [cm]	Z' [cm]	E [MPa]
15	16	4	3857.81	15	10	1	15,822.69
30	19.5	7.5	4115.00	30	11	2	15,822.69
50	24.5	12.5	4115.00	50	14	5	10,548.46
65	27	15	4457.92	65	17.5	8.5	8066.47
80	30	18	4572.22	80	20	11	7671.61
		\bar{E}	4223.59	95	23	14	7157.88
		σ	288.89	110	26	17	6825.47
		μ	6.84	140	31.5	22.5	6563.49
				170	39	30	5977.46
						\bar{E}	9384
						σ	3873
						μ	41.27

* where G —total weight of the weights; L —length of the branch; d_k —thicker (final) diameter of the branch; d_p —thinner (initial) diameter of the branch; Z_o —position of the unloaded branch as read from the scale; Z —position of the loaded branch as read from the scale (Figure 7); Z' —the value of the deflection arrow $Z' = Z - Z_o$; E —elasticity modulus determined from relation (17).

Table 6. Summary of the calculated modulus of elasticity for individual branches of shrub No. 1 under the vegetation and non-vegetation period.

Branch Number (-)	Under Vegetation Conditions					Non-Vegetation Conditions				
	\bar{E} (MPa)	Standard Deviation σ (MPa)	Coefficient of Variation μ (%)	Min \bar{E} (MPa)	Max E (MPa)	\bar{E} (MPa)	Standard Deviation σ (MPa)	Coefficient of Variation μ (%)	Min E (MPa)	Max E (MPa)
1	4224	289	6.84	3858	4572	9384	3873	41.27	5977	15,823
2	2968	653	22.0	2456	3703	4886	789	16.1	3837	5627
3	1605	77	4.8	1551	1659	2207	138	6.3	2045	2374
4	4142	574	13.9	3572	4719	8486	1084	12.8	7292	10,354
5	1673	100	6.0	1486	1776	2389	985	41.3	1796	4755
6	1181	214	18.1	870	1334	1632	173	10.6	1420	1893
7	660	117	17.8	509	805	1166	125	10.7	869	1288
8	1413	159	11.2	1230	1515	1254	182.3	14.5	1086	1448

Figure 9 shows the deflection arrow values of selected branches loaded at 50 cm above ground level for three shrubs during the vegetation and non-vegetation seasons.

Branch No. 10 and 16 (shrub 2 and shrub 3, respectively), both in the vegetation and non-vegetation seasons, were characterised by the highest stiffness. The maximum deflection, for a load of 430 g, did not exceed 30 cm. However, it should be noted that these were the thickest branches on which measurements were carried out, with diameters of 10.55 and 20.3 mm, respectively, and were characterised by the greatest lignification. This had the effect of increasing the mechanical strength of the branches, as well as the resistance to compression and, in part, frost resistance [42]. In the case of branches 3 and 2 (shrub 1), the deflections were more than 40 cm and already at low loads of 30–65 g. These branches were characterised by a small diameter of 4.94 and 8.68 mm at the thickest point, respectively, and with practically no lignification. These were young, annual shoots.

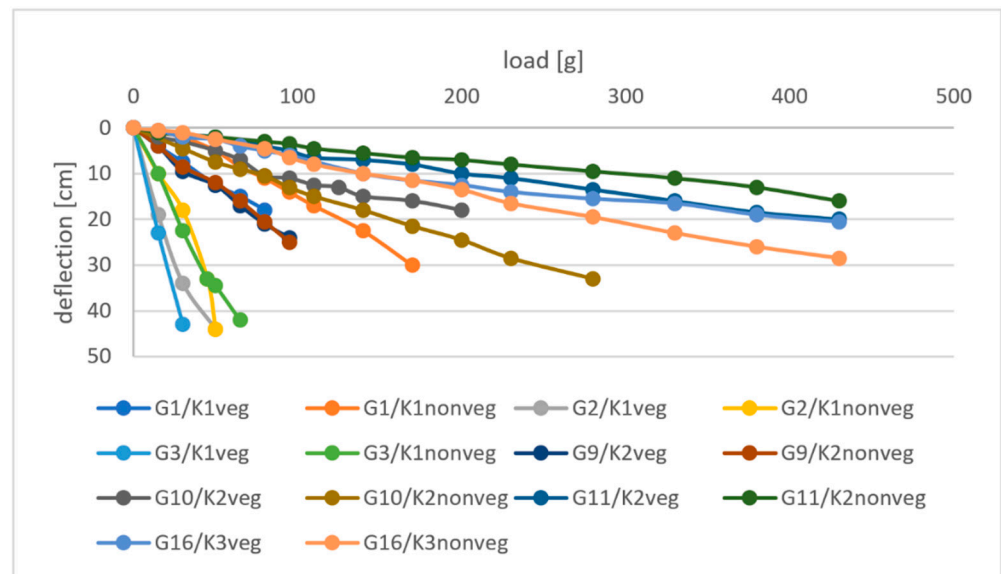


Figure 9. Figures of deflection arrows of selected branches of shrubs 1, 2, and 3, loaded at 50 cm above ground level (where Gx—branch number; Kx—shrub number).

The branches of shrubs 1 and 2 loaded at a height of 100 cm from the surface were characterised by small diameters ranging from about 2.5 to 5.2 mm at their thinnest point to about 12 mm at their thickest point. They therefore flexed significantly already at weights that did not exceed 100 g (Figure 10). Only the branches of shrub No. 3, even with a load of 500 g, were deflected to a maximum of 25 cm. The results obtained may also be influenced by the shrub species. Shrub 1 is an example of brittle willow (*Salix fragilis*), shrub 2 is basket willow (*Salix viminalis* L.) and shrub 3 is white willow (*Salix alba*).

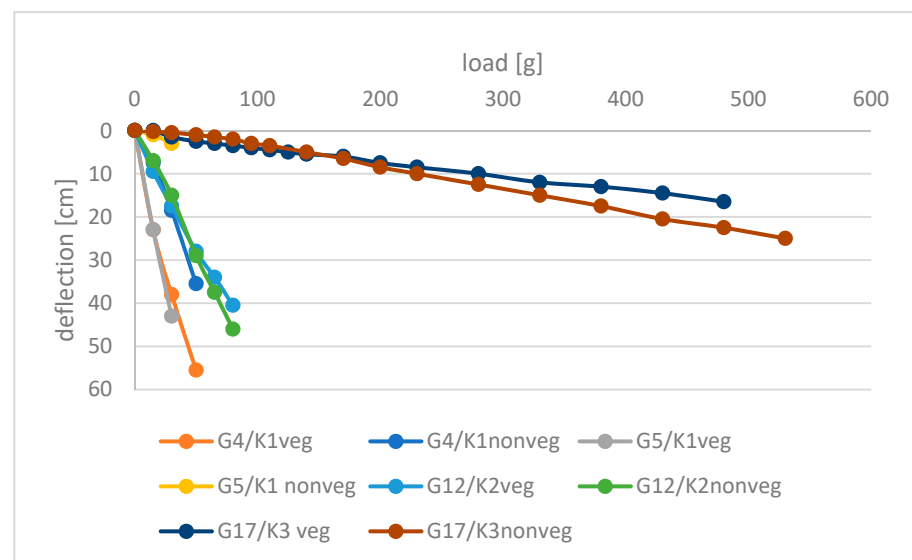


Figure 10. Figures of deflection arrows of selected branches of shrubs 1, 2, and 3, loaded at 100 cm above ground level (where Gx—branch number; Kx—shrub number).

The branches loaded at a height of 150 cm from the surface (Figure 11) had the smallest diameters ranging from 2.94 at the narrowest point to 11.5 mm at the thickest point; only branch No. 14 at the thickest point was 13.2 mm (average 5.5 mm) during the vegetation and the non-vegetation period. At this height in the plant, there is mainly meristem (growth cone)—which is made up of small cells with a significant rate of division. There is little or no lignification. As a result of these divisions, the shoot grows in length and there is

only a small primary increment in thickness. Therefore, significant deflection values were recorded of up to 95 cm, even with a relatively low load of around 100 g (Figure 11). The branches with the highest deflection (Nos. 6, 13, 15) were relatively young shoots with diameters of 8.3, 11.6 and 9.0 mm, respectively. The older branch, for example 17, had up to four times less deflection even at five times the load, despite a diameter of about 8 mm.

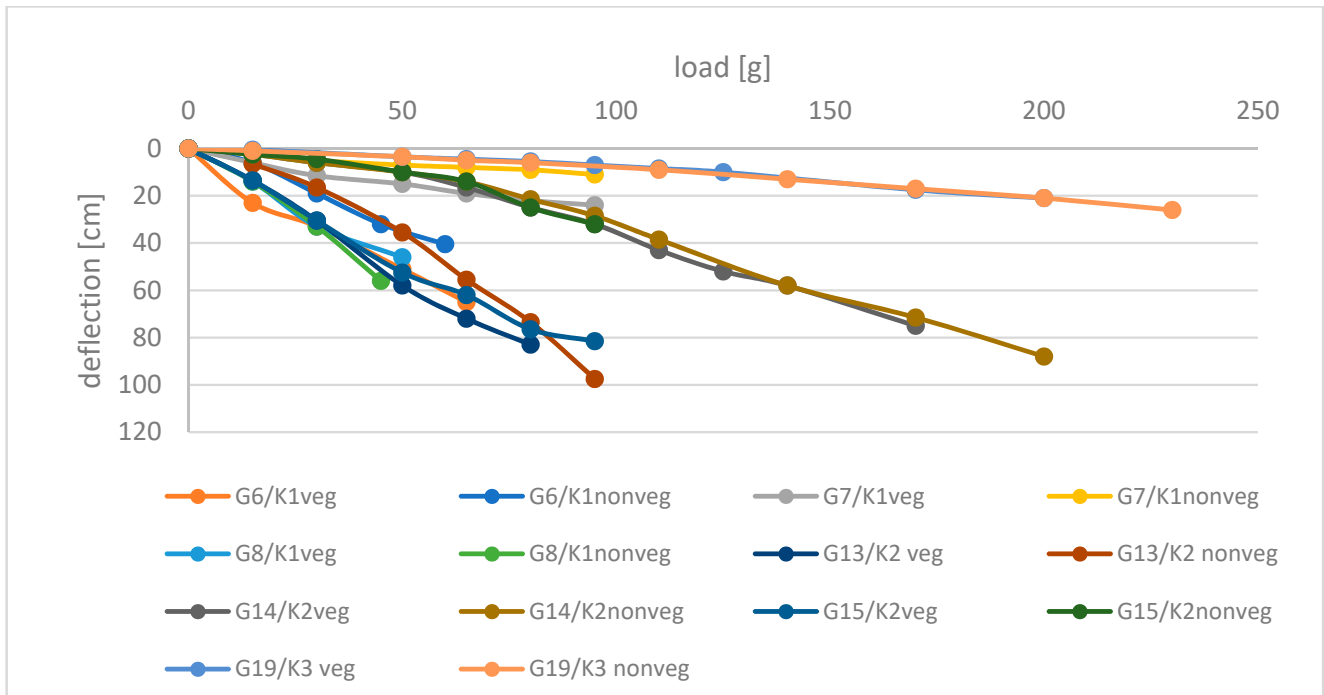


Figure 11. Figures of deflection arrows of selected branches of shrubs 1, 2, and 3, loaded at 150 cm above ground level (where Gx—branch number; Kx—shrub number).

The deflection arrow values during the conducted experiments were significantly lower in the non-vegetation period for shrub No. 1, comparing the analogously applied load, and it took a higher load to achieve similar deflection arrow values in the winter compared to the growing season. In the winter season, the values were lower, from several cm to as much as 20 cm. The greatest differences were recorded on the thinnest branches, with an average diameter of less than 4 mm. For branches with an average diameter of 5–6 mm, smaller deflection arrows of about 13–16 mm were observed in the non-vegetation season. For larger diameters, the differences in deflection arrows were even smaller and did not exceed 7.5 mm.

In the case of shrubs 2 and 3, the situation is no longer so clear-cut. The differences in the values of the deflection arrow for individual branches loaded with the same values are already much smaller. They oscillate between 0.5 and 2 cm, and in most cases do not exceed about 6 cm. The exceptions are branches 13 and 15 for shrub No. 2, for which changes above 20 cm were recorded (smaller arrows in the winter season).

3.3. Modulus of Elasticity

Based on the measured values of deflection, the modulus of elasticity for individual branches was determined from Equation (17). Table 5 shows, for example, the modulus of elasticity of branch No. 1 in a shrub loaded at the height of 50 cm from the ground level. The averaged values of the modulus of elasticity for the analysed shrubs are summarised in Tables 6–8. Analysing the results obtained for all the branches of shrub 1, it is possible to observe (for most branches) an increase in the average modulus of elasticity in the winter period, even more than twice that in the cases of branches 1 and 4. For the remaining branches, the increase in modulus of elasticity ranged from 30 to about 75%. The exception

is branch 8, where a slight decrease in the modulus of elasticity was recorded. Shrub 1, brittle willow (*Salix fragilis*), showed the greatest variation in the mean value of elastic modulus for almost all of the branches (Table 6).

Table 7. Summary of calculated modulus of elasticity for individual branches of shrub No. 2 under vegetation and non-vegetation conditions.

Branch Number (-)	Under Vegetation Conditions					Non-Vegetation Conditions				
	\bar{E} (MPa)	Standard Deviation σ (MPa)	Coefficient of Variation. μ (%)	Min E (MPa)	Max E (MPa)	\bar{E} (MPa)	Standard Deviation σ (MPa)	Coefficient of Variation μ (%)	Min E (MPa)	Max E (MPa)
9	4493	632	14.07	3773	5660	4309	230	5.35	3995	4717
10	2338	270	11.6	1875	2777	1912	222	11.6	1641	2462
11	1091	184	16.9	844	1496	1072	147	13.7	626	1252
12	2856	251	8.8	2515	3146	2550	271	10.6	2323	2987
13	1399	186	13.3	1219	1697	1846	657	35.6	1237	2929
14	5426	2552	47.0	3650	12,077	5793	2341	40.4	3413	10,010
15	1117	85	7.6	1005	1231	2238	754	33.7	1316	3373

Table 8. Summary of calculated modulus of elasticity for individual branches of shrub No. 3 under vegetation and non-vegetation conditions.

Branch Number (-)	Under Vegetation Conditions					Non-Vegetation Conditions				
	\bar{E} (MPa)	Standard Deviation σ (MPa)	Coefficient of Variation. μ (%)	Min E (MPa)	Max E (MPa)	\bar{E} (MPa)	Standard Deviation σ (MPa)	Coefficient of Variation μ (%)	Min E (MPa)	Max E (MPa)
16	2604	398	15.29	2104	3310	2558	721.2	28.20	2052	4477
17	878	878	12.1	676	1014	825	322.0	39.0	569	1627
18	1339	1339	7.8	1187	1582	1636	399.4	24.4	1231	2535
19	4830	4830	39.3	3215	10,214	3424	683.7	20.0	2368	4314

For shrubs No. 2 and No. 3 belonging to the species of the Basket Willow (*Salix viminalis*) and the White Willow (*Salix alba*), respectively, for the majority of branches no clear effect of the study period on the stiffness of their branches is observed. Small decreases in the average modulus of elasticity in the non-vegetation period are recorded, ranging from a few to about 10%. The exceptions here are branches 13 and 15 of shrub No. 2, similar to the case of the deflection arrow. Under non-vegetative conditions, the value of the average modulus of elasticity for these shrubs decreased slightly compared to the vegetative period. Some shoots showed higher stiffness under non-vegetation conditions, but for most this value was lower or without significant changes (Tables 7 and 8).

The determined elastic modulus \bar{E} for all analysed branches ranged from 660 to 9384 MPa, $\bar{E} = 2784$ MPa, SD = 2002 MPa.

4. Discussion

To determine the effect of weather conditions on changes in branch stiffness, data were compared from two periods: vegetation and non-vegetation. Under vegetation conditions, the mean values of the modulus of elasticity ranged from approximately 2200 MPa to approximately 2700 MPa. The highest mean modulus of elasticity of 2674 MPa was recorded for the shrub 2 *Salix viminalis*, the lowest 2233 MPa for the shrub 1 *Salix fragilis*. Shrub 2 and 3 were also characterised by the highest variation of mean modulus, as the standard deviation of the modulus of elasticity was at the level of 1700 MPa. The results presented from the elastic modulus tests (Tables 6–8) indicate a high natural variability of the mechanical parameters even within the same plant. In the non-vegetation period, the highest elastic modulus was recorded for shrub 1, recording a 1.5-fold increase compared to the growing period. Similar results were obtained by Beismann et al., [43], who measured the elastic modulus of branches of four willow species: *Salix alba*, *Salix Rubens*, *Salix fragilis*, and *Salix appendiculata* under laboratory conditions. The results of their study are also

characterised by high variability, reaching a max. of 4000 MPa. The analyses carried out showed that the maximum standard deviation of the modulus of elasticity, in the non-vegetation period, was as high as 3300 MPa for shrub 1.

In a study conducted by Tymiński et al. [31,44] on branches of, among others, purple willow (*Salix purpurea*) under laboratory conditions, the measured elastic modulus of fresh branches ranged between 4000–4500 MPa, while for dry branches an average modulus value of approximately 7300–8900 MPa was obtained.

Stone, et al. [3] conducted a study of the behaviour of woody vegetation to changing hydraulic flow conditions under natural conditions. Their analyses were used to predict tree bending at water velocities (0.5, 1.0, 1.5, 2.0 and 2.5 m·s⁻¹) likely to occur during floods. The bending simulations revealed considerable variability, taking into account the geometrical parameters of the plants as well as their individual biomechanical characteristics resulting from specific species. An averaged modulus of elasticity of 3323 MPa was obtained for a willow with an average height (from 12 plants) of 5.6 m.

Tan et al. [45] in their study also determined the rigidity modulus using Equation (17), and it ranged from 110 to 16,560 MPa. The purpose of the experiment was to determine the effect of plant rigidity on the wave dissipation and turbulence process. For this purpose, the researchers used four groups of rods with different stiffness that simulated natural vegetation. Tan et.al observed that the change in turbulence intensity in different groups of rods depends on the rigidity, and the higher the rigidity of the rod, the higher the turbulence intensity.

Luhar et al. [46] demonstrated in their laboratory study using seagrass (*Zostera marina*) that a simple model that balances the effect of hydrodynamic drag with restoring forces (due to vegetation stiffness and buoyancy) can be successfully used to model deflection and drag for both artificial and natural aquatic vegetation. The study confirmed that the analysed fully submerged elastic vegetation has a modulus of elasticity in the range between 400 and 2400 MPa.

Modelling studies using seagrass were also carried out by Nakayama et al. [47], who evaluated the bidirectional effects of plant-flow interaction under laboratory conditions. To capture multiphase phenomena, an approach was used in which submerged vegetation is described by the discrete element method and is combined with a flow dynamics model to resolve stresses from streams and waves.

The influence of hydrological conditions on the bending stiffness of floodplain vegetation represented by trees (poplars) was also addressed by Niez, et al. [48], who investigated over a period of five months whether periodic and controlled deflections affect the mechanical properties of plants growing under windy conditions. The analysis was extended to vegetation development (i.e., change in geometric dimensions) under well-watered conditions and hydrological stress. The results indicate a strong influence of tigmomorphogenesis on growth processes, even underwater deficit conditions. Plants (vertical) did not develop properly due to mechanical stimulation and hydrological stress. In contrast, radial growth was enhanced by the periodic bending of shoots, leading to ovalization of the cross-section. This ovalization, regardless of hydrological conditions, was responsible for an increase of 16% in radial biomass and an increase in tree bending stiffness of up to 212%.

The stiffness of individual submerged vegetation species under laboratory conditions was also studied by Wu and Yang [49]. They obtained a mathematical model that describes the relative stiffness for bending submerged vegetation. In addition, they observed that the relative bending stiffness of submerged vegetation, which was placed in the central part of the channel, decreases with the hydraulic changes of the flow (Reynolds and Froude numbers) and increases with the increase of the cross-sectional aspect ratio. For different water table levels, Wu and Yang [49] obtained stiffness limits from which they determined whether the submerged vegetation could be considered fully elastic or fully rigid.

5. Conclusions

Vegetation dynamics can vary greatly along a river where water flow, gradient and grain size are essentially constant. Bertoldi et al. [18] in their study found morphological changes in almost 60% of the active corridor area which were associated with a reduction in the area covered by vegetation in the most highly vegetated subsections from over 30% to about 23%. The authors also found that faster tree growth not only directly promotes biomass development and an increase in the area covered by vegetation, but when sampling trees 2.5–3.5 m tall, they observed that fast-growing trees have more flexible trunks than slower-growing trees of the same height, which may provide the former with a greater ability to flex during flooding and thus resist uprooting and rapidly regenerate after flood flows. The researchers confirmed that in the sectors where vegetation growth was fastest and the area of vegetation was greatest, the early period of vegetation expansion was accompanied by an increase in the number of vegetation-covered areas, but once the area of vegetation exceeded 10%, these areas began to merge and decrease in number. This contrasts with the upstream and downstream sectors, where tree growth rates are lower, vegetation cover is lower, and the area and number of vegetation-covered areas continued to increase during the early period of vegetation expansion. Subareas containing higher vegetation also showed higher mean vegetation density (Spearman rank correlation = 0.753, $p < 0.001$). All these correlations illustrate that the studied section provides large contrasts in tree cover, height and density [19]. Tree increments were about 30–40 cm/year.

Smaller plants, mainly individuals of the *Salix* species, on surfaces exposed to more frequent and damaging stress during floods find it more difficult to recover between floods [20], while more protected sites on floodplains provide better conditions for plants to germinate and grow. The behaviour of vegetation was determined by the timing of wave passage, the age and flexibility (vitality) of vegetation, the morphological shape of the valley and the intensity of flooding. Džubáková et al. [20] found that vegetation in a river environment with a highly variable surface area differed in the direction of predicted changes and their spatial distribution in the range 0.7–35.8%.

Errico et al. [22] indicate that under fully vegetated channel conditions, flow resistance showed a decreasing trend with increasing flows, indicating that the presence of spontaneous vegetation increased channel roughness by a factor of four compared to the scenario without vegetation. For the scenario with a partially vegetated channel, flow resistance was lower because a larger portion of the channel cross-section was cleared by partial cutting. The roughness coefficients were approximately 50% higher than the roughness values of the scenario for the channel without vegetation. The fully cleared scenario had the lowest Manning coefficients for all discharges, with values comparable to those proposed in the literature for regular channels with a natural bed. An important observation during the field study conducted by [22] was the behaviour of the vegetation elements during bending. It was found that the reconfiguration and bending of plants caused by flow action on stems and leaves leads to a significant reduction in flow resistance. Consequently, the bending of flexible plant elements significantly affects the Manning's n roughness, which decreases with increasing VR (V is the flow velocity, R is the hydraulic radius) and tends to a constant value when the water depth is equal to or greater than five times the height of the bent vegetation. Moreover, the area occupied by plants decreased with increasing flow rate. This can be explained by a partial reconfiguration of the leaves, which began to bend as water velocity and depth increased.

Changes in diameters and deflection values of selected branches of three shrubs (*Salix fragilis*, *Salix viminalis* L. and *Salix alba*) loaded at three heights (50, 100 and 150 cm) in different growth periods (vegetation and post-vegetation) were analysed under field conditions. The elasticity modulus E of the branches was also estimated based on the performed measurements. The mean modulus of elasticity for *Salix fragilis* (shrub 1) was 2233 and 3313 MPa for the vegetation and non-vegetation seasons, respectively, which corresponds to an increase in stiffness of about 1.5 times in the non-vegetation season relative to branch stiffness in the growing season. For shrub 2, the mean modulus of

elasticity practically did not change with the change in period and was 2674 and 2817 MPa for the vegetation and non-vegetation seasons, respectively. For shrub 3, there was a slight 3% decrease in the mean modulus of elasticity from 2413 and 2111 MPa for the vegetation and non-vegetation conditions, respectively. However, it is important to note the high variability in both diameters and elastic moduli within the same shrub. This is evidenced by the coefficients of variation, which is very high in the case of change in mean diameter between measurement periods, which is, of course, understandable due to the growth of shrubs, but also by quite high coefficients of variation in elastic modulus, reaching up to almost 50% within a given measurement series.

The research presented herein is in line with and an extension of laboratory studies conducted by other researchers. The results obtained in this paper correspond to previously cited results. However, different from the cited works based primarily on laboratory measurements, the present results are based on studies conducted in situ on natural shrubby vegetation. The study was conducted in three different vegetation periods, which made it possible to estimate changes in plant flexibility and diameter changes in relation to plant growth.

Author Contributions: Conceptualization, N.W.; methodology, N.W. and Z.W.; validation, N.W., T.F. and Z.W.; formal analysis, N.W., T.F. and Z.W.; investigation, N.W., Z.W. and T.F.; writing—original draft preparation, N.W. and Z.W.; writing—review and editing, N.W. and Z.W.; visualization, Z.W. and T.F. All authors have read and agreed to the published version of the manuscript.

Funding: The publication was co-financed within the framework of Ministry of Science and Higher Education program as “Regional Initiative Excellence” in years 2019–2022, Project No. 005/RID/2018/19.

Institutional Review Board Statement: Not applicable.

Informed Consent Statement: Not applicable.

Data Availability Statement: Not applicable.

Conflicts of Interest: The authors declare that they have no conflict of interest.

References

1. Prus, P.; Popek, Z.; Pawlaczyk, P. *Good River Maintenance Practices*; WWF Polska: Warsaw, Poland, 2018; ISBN 836206949X. (In Polish)
2. Walczak, N.; Hämmerling, M.; Szymczak-Graczyk, A. Agricultural use of floodplains above Jeziorsko Reservoir. *Inżynieria Ekol.* **2017**, *18*, 225–233. (In Polish) [[CrossRef](#)]
3. Stone, M.C.; Chen, L.; Kyle McKay, S.; Goreham, J.; Acharya, K.; Fischenich, C.; Stone, A.B. Bending of submerged woody riparian vegetation as a function of hydraulic flow conditions. *River Res. Appl.* **2013**, *29*, 195–205. [[CrossRef](#)]
4. Kubrak, J.; Nachlik, E. *Hydraulic Basis for Calculating the Capacity of River Channels*; SGGW: Warsaw, Poland, 2003; ISBN 8372443858. (In Polish)
5. Szoszkiewicz, K.; Jusik, S.; Zgoła, T. *Key to the Determination of Macrolites for the Assessment of the Ecological Status of Surface Waters*; Inspekcja Ochrony Środowiska: Warsaw, Poland, 2010; ISBN 8361227326. (In Polish)
6. Greiner, J.T.; McGlathery, K.J.; Gunnell, J.; McKee, B.A. Seagrass restoration enhances “blue carbon” sequestration in coastal waters. *PLoS ONE* **2013**, *8*, e72469. [[CrossRef](#)] [[PubMed](#)]
7. Tang, J.; Ye, S.; Chen, X.; Yang, H.; Sun, X.; Wang, F.; Wen, Q.; Chen, S. Coastal blue carbon: Concept, study method, and the application to ecological restoration. *Sci. China Earth Sci.* **2018**, *61*, 637–646. [[CrossRef](#)]
8. Arkema, K.K.; Griffin, R.; Maldonado, S.; Silver, J.; Suckale, J.; Guerry, A.D. Linking social, ecological, and physical science to advance natural and nature-based protection for coastal communities. *Ann. N. Y. Acad. Sci.* **2017**, *1399*, 5–26. [[CrossRef](#)] [[PubMed](#)]
9. Barbier, E.B.; Georgiou, I.Y.; Enchelmeier, B.; Reed, D.J. The value of wetlands in protecting southeast Louisiana from hurricane storm surges. *PLoS ONE* **2013**, *8*, e58715. [[CrossRef](#)]
10. Costanza, R.; d’Arge, R.; de Groot, R.; Farber, S.; Grasso, M.; Hannon, B.; Limburg, K.; Naeem, S.; O’neill, R.V.; Praelo, J. The value of the world’s ecosystem services and natural capital. *Nature* **1997**, *387*, 253–260. [[CrossRef](#)]
11. Waycott, M.; Longstaff, B.J.; Mellors, J. Seagrass population dynamics and water quality in the Great Barrier Reef region: A review and future research directions. *Mar. Pollut. Bull.* **2005**, *51*, 343–350. [[CrossRef](#)]
12. Duan, J.G.; Barkdoll, B.; French, R. Lodging velocity for an emergent aquatic plant in open channels. *J. Hydraul. Eng.* **2006**, *132*, 1015–1020. [[CrossRef](#)]
13. Schutten, J.; Dainty, J.; Davy, A.J. Root anchorage and its significance for submerged plants in shallow lakes. *J. Ecol.* **2005**, *93*, 556–571. [[CrossRef](#)]

14. Sand-Jensen, K. Drag and reconfiguration of freshwater macrophytes. *Freshw. Biol.* **2003**, *48*, 271–283. [[CrossRef](#)]
15. WU, F.; JIANG, S.; YANG, X. Characteristics of 2D-vortex field in open channel flow with submerged rigid vegetation. *Chin. J. Hydrodyn.* **2010**, *25*, 8–15.
16. Laounia, N.; Zhongmin, Y.; Ji-hong, X.I. Study of the flow through non-submerged vegetation. *J. Hydrodyn.* **2005**, *17*, 498–502.
17. Wang, P.; Wang, C.; Zhu, D.Z. Hydraulic resistance of submerged vegetation related to effective height. *J. Hydrodyn.* **2010**, *22*, 265–273. [[CrossRef](#)]
18. Bertoldi, W.; Drake, N.A.; Gurnell, A.M. Interactions between river flows and colonizing vegetation on a braided river: Exploring spatial and temporal dynamics in riparian vegetation cover using satellite data. *Earth Surf. Process. Landf.* **2011**, *36*, 1474–1486. [[CrossRef](#)]
19. Bertoldi, W.; Gurnell, A.M.; Drake, N.A. The topographic signature of vegetation development along a braided river: Results of a combined analysis of airborne lidar, color air photographs, and ground measurements. *Water Resour. Res.* **2011**, *47*. [[CrossRef](#)]
20. Džubáková, K.; Molnar, P.; Schindler, K.; Trizna, M. Monitoring of riparian vegetation response to flood disturbances using terrestrial photography. *Hydrol. Earth Syst. Sci.* **2015**, *19*, 195–208. [[CrossRef](#)]
21. Apollonio, C.; Petroselli, A.; Cornelini, P.; Manzari, V.; Preti, F.; Grimaldi, S. Riparian vegetation as a marker for bankfull and management discharge evaluation: The case study of Rio Torbido river basin (central Italy). *J. Agric. Eng.* **2021**, *52*. [[CrossRef](#)]
22. Errico, A.; Pasquino, V.; Maxwald, M.; Chirico, G.B.; Solari, L.; Preti, F. The effect of flexible vegetation on flow in drainage channels: Estimation of roughness coefficients at the real scale. *Ecol. Eng.* **2018**, *120*, 411–421. [[CrossRef](#)]
23. Zhang, X.; Nepf, H. Flow-induced reconfiguration of aquatic plants, including the impact of leaf sheltering. *Limnol. Oceanogr.* **2020**, *65*, 2697–2712. [[CrossRef](#)]
24. Vogel, S. Drag and reconfiguration of broad leaves in high winds. *J. Exp. Bot.* **1989**, *40*, 941–948. [[CrossRef](#)]
25. Xavier, P.; Wilson, C.; Aberle, J.; Rauch, H.P.; Schoneboom, T.; Lammeranner, W.; Thomas, H. Drag Force of Flexible Submerged Trees. In Proceedings of the HYDRALAB III Joint User Meeting, Hannover, Germany, 2–4 February 2010.
26. Jalonen, J.; Järvelä, J. Impact of tree scale on drag: Experiments in a towing tank. In Proceedings of the 35th IAHR World Congress, Chengdu, China, 8–13 September 2013; pp. 1–12.
27. Whittaker, P.; Wilson, C.; Aberle, J.; Rauch, H.P.; Xavier, P. A drag force model to incorporate the reconfiguration of full-scale riparian trees under hydrodynamic loading. *J. Hydraul. Res.* **2013**, *51*, 569–580. [[CrossRef](#)]
28. Västilä, K.; Järvelä, J. Modeling the flow resistance of woody vegetation using physically based properties of the foliage and stem. *Water Resour. Res.* **2014**, *50*, 229–245. [[CrossRef](#)]
29. Henry, H.A.L.; Thomas, S.C. Interactive effects of lateral shade and wind on stem allometry, biomass allocation, and mechanical stability in *Abutilon theophrasti* (Malvaceae). *Am. J. Bot.* **2002**, *89*, 1609–1615. [[CrossRef](#)]
30. Li, Y.-H.; Xie, L.; Su, T. Resistance of open-channel flow under the effect of bending deformation of submerged flexible vegetation. *J. Hydraul. Eng.* **2018**, *144*, 4017072. [[CrossRef](#)]
31. Tymiński, T.; Rembeza, L.; Kałuża, T. *Analysis of Impact of Flexible Vegetation on Hydraulic Conditions of Flow in Vegetated Channels. Part 1: MECHANICAL Properties of Elastic Plants*, 1st ed.; Tymiński, T., Ed.; UPWr: Wrocław, Poland, 2008; ISBN 978-83-60574-18-8. (In Polish)
32. Irvine, J.; Grace, J. Continuous measurements of water tensions in the xylem of trees based on the elastic properties of wood. *Planta* **1997**, *202*, 455–461. [[CrossRef](#)]
33. Cochard, H.; Lemoine, D.; Améglio, T.; Granier, A. Mechanisms of xylem recovery from winter embolism in *Fagus sylvatica*. *Tree Physiol.* **2001**, *21*, 27–33. [[CrossRef](#)]
34. Zürcher, E.; Cantiani, M.-G.; Sorbetti-Guerri, F.; Michel, D. Tree stem diameters fluctuate with tide. *Nature* **1998**, *392*, 665–666. [[CrossRef](#)]
35. Auchmoody, L.R. *Epicormic Branching: Seasonal Change, Influence of Fertilization, and Frequency of Occurrence in Uncut Stands*; Northeastern Forest Experiment Station, Forest Service, U.S. Department of Agriculture: Upper Darby, PA, USA, 1972.
36. Améglio, T.; Bodet, C.; Lacoïnte, A.; Cochard, H. Winter embolism, mechanisms of xylem hydraulic conductivity recovery and springtime growth patterns in walnut and peach trees. *Tree Physiol.* **2002**, *22*, 1211–1220. [[CrossRef](#)]
37. Zweifel, R.; Häsler, R. Frost-induced reversible shrinkage of bark of mature subalpine conifers. *Agric. For. Meteorol.* **2000**, *102*, 213–222. [[CrossRef](#)]
38. Walczak, N.; Walczak, Z.; Kałuża, T.; Hämmerling, M.; Stachowski, P. The Impact of shrubby floodplain vegetation Growth on the discharge capacity of river valleys. *Water* **2018**, *10*, 556. [[CrossRef](#)]
39. Otepka, P.; Habán, M.; Habánová, M. Cultivation of fast-growing woody plant basket willow (*Salix viminalis* L.) and their bioremedial abilities while fertilized with wood ash. *Res. J. Agric. Sci.* **2011**, *43*, 218–222.
40. Stolarski, M.J.; Szczukowski, S.; Tworkowski, J.; Klasa, A. Willow biomass production under conditions of low-input agriculture on marginal soils. *For. Ecol. Manag.* **2011**, *262*, 1558–1566. [[CrossRef](#)]
41. Donaldson, L.A. Lignification and lignin topochemistry—An ultrastructural view. *Phytochemistry* **2001**, *57*, 859–873. [[CrossRef](#)]
42. Boudet, A.-M. Lignins and lignification: Selected issues. *Plant Physiol. Biochem.* **2000**, *38*, 81–96. [[CrossRef](#)]
43. Beismann, H.; Wilhelmi, H.; Baillères, H.; Spatz, H.-C.; Bogenrieder, A.; Speck, T. Brittleness of twig bases in the genus *Salix*: Fracture mechanics and ecological relevance. *J. Exp. Bot.* **2000**, *51*, 617–633. [[CrossRef](#)]
44. Tymiński, T.; Kałuża, T. Investigation of mechanical properties and flow resistance of flexible riverbank vegetation. *Pol. J. Environ. Stud.* **2012**, *21*, 201–207.

45. Tan, C.; Huang, B.; Liu, D.; Qiu, J.; Chen, H.; Li, Y.; Hu, Z. Effect of mimic vegetation with different stiffness on regular wave propagation and turbulence. *Water* **2019**, *11*, 109. [[CrossRef](#)]
46. Luhar, M.; Nepf, H.M. Flow-induced reconfiguration of buoyant and flexible aquatic vegetation. *Limnol. Oceanogr.* **2011**, *56*, 2003–2017. [[CrossRef](#)]
47. Nakayama, K.; Shintani, T.; Komai, K.; Nakagawa, Y.; Tsai, J.-W.; Sasaki, D.; Tada, K.; Moki, H.; Kuwae, T.; Watanabe, K. Integration of submerged aquatic vegetation motion within hydrodynamic models. *Water Resour. Res.* **2020**, *56*, e2020WR027369. [[CrossRef](#)]
48. Niez, B.; Dlouha, J.; Moulia, B.; Badel, E. Water-stressed or not, the mechanical acclimation is a priority requirement for trees. *Trees* **2019**, *33*, 279–291. [[CrossRef](#)]
49. Wu, L.; Yang, X. Factors influencing bending rigidity of submerged vegetation. *J. Hydrodyn.* **2011**, *23*, 723–729. [[CrossRef](#)]